

*Supplementary Information*

**Physical Exfoliation of Graphene and Molybdenum Disulfide Sheets  
Using Conductive Polyaniline: An Efficient Route for Synthesizing  
Unique, Random-Layered 3D Ternary Electrode Materials**

Seonmyeong Noh,<sup>a</sup> Thanh-Hai Le,<sup>b</sup> Chul Soon Park,<sup>b</sup> Saerona Kim,<sup>b</sup> Yukyung Kim,<sup>b</sup>  
Jong-Jin Park,<sup>a,b</sup> and Hyeonseok Yoon<sup>a,b,\*</sup>

<sup>a</sup>Alan G. MacDiarmid Energy Research Institute, School of Polymer Science and Engineering,  
Chonnam National University, 77 Yongbong-ro, Buk-gu, Gwangju 61186, South Korea.

<sup>b</sup>Department of Polymer Engineering, Graduate School, Chonnam National University,  
77 Yongbong-ro, Buk-gu, Gwangju 61186, South Korea.

Corresponding Authors:

\*E-mail: hyoon@chonnam.ac.kr

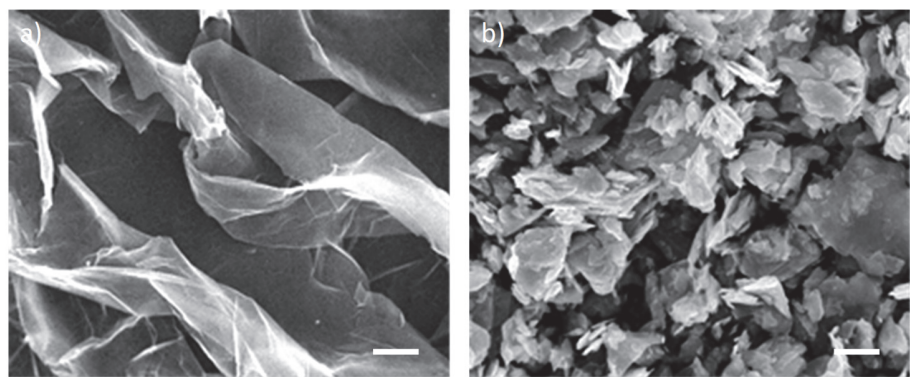


Figure S1. Typical SEM images of (a) graphene and (b) MoS<sub>2</sub> (scale bar: 2 μm).

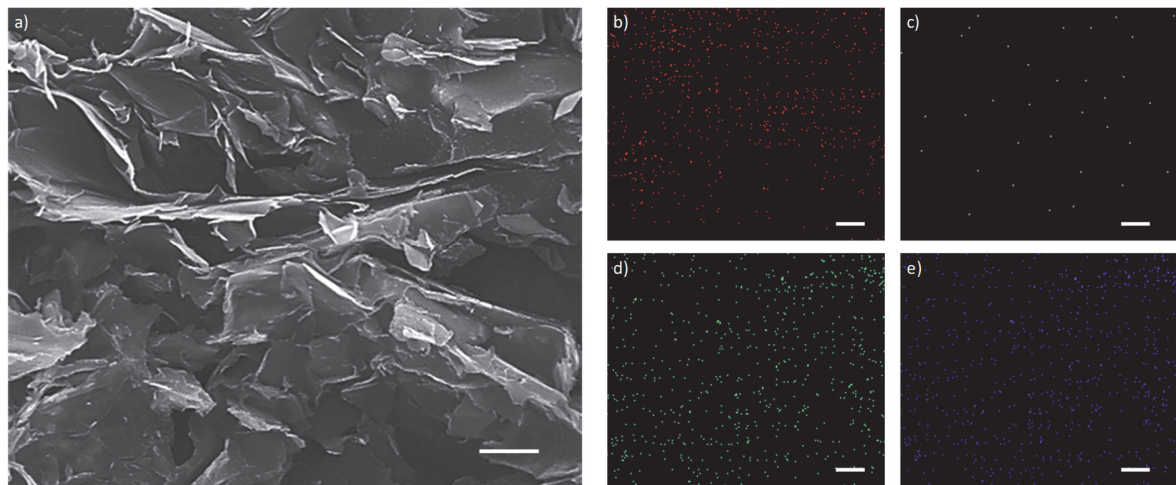


Figure S2. SEM image of GMPN and its mapping images indicating individual components: (a) typical SEM image and mapping images of (b) carbon, (c) nitrogen, (d) molybdenum, and (e) sulfur (scale bar: 2  $\mu$ m).

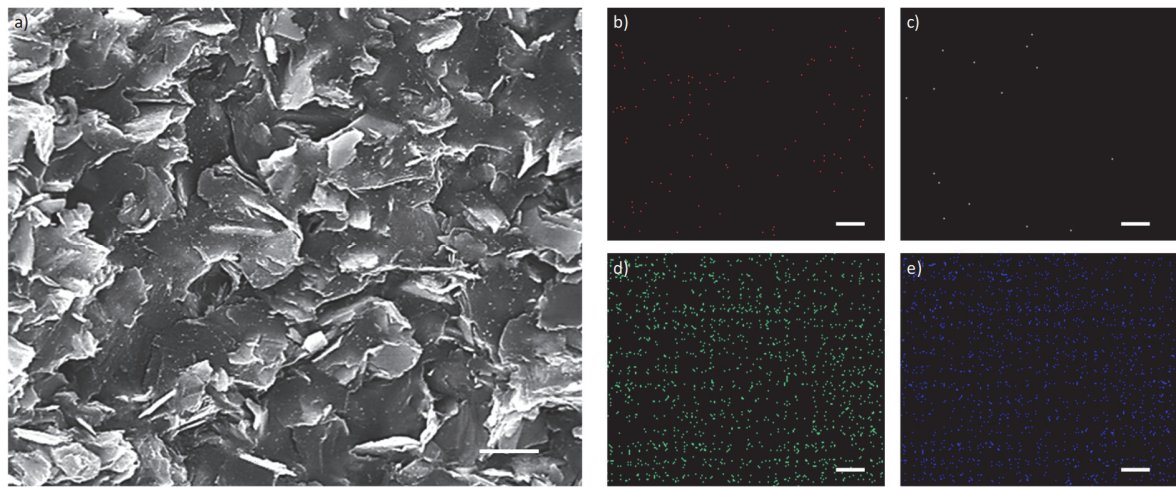


Figure S3. SEM image of MPN and its mapping images indicating individual components: (a) typical SEM image and mapping images of (b) carbon, (c) nitrogen, (d) molybdenum, and (e) sulfur (scale bar: 2  $\mu\text{m}$ ).

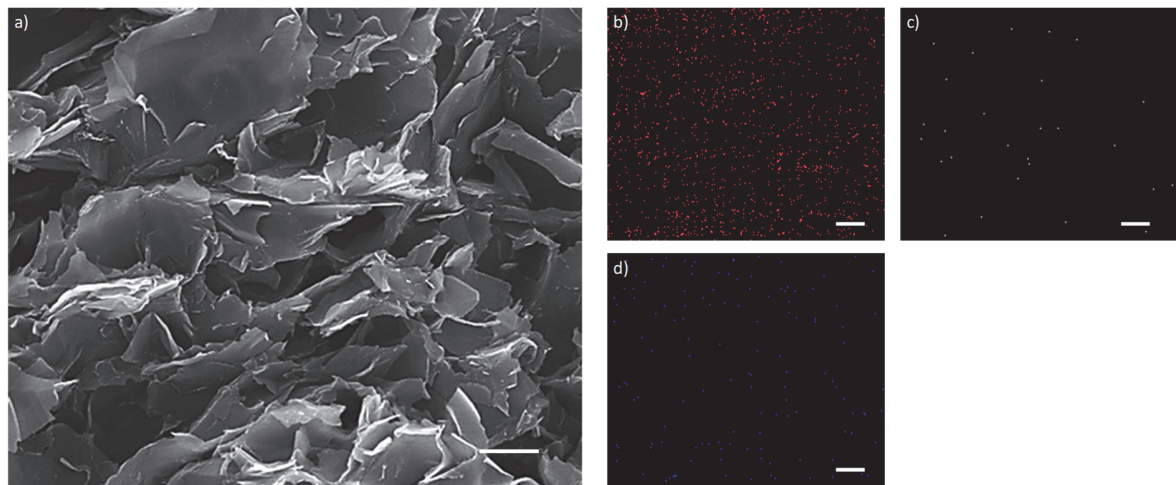


Figure S4. SEM image of GPN and its mapping images indicating individual components: (a) typical SEM image and mapping images of (b) carbon, (c) nitrogen, and (d) sulfur (scale bar: 2  $\mu\text{m}$ ).

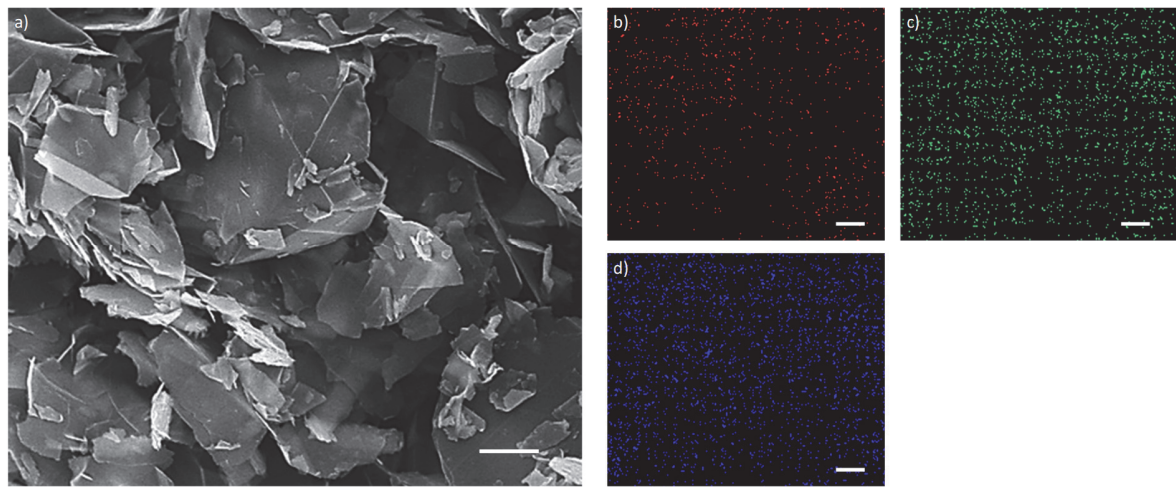


Figure S5. SEM image of GMN and its mapping images indicating individual components: (a) typical SEM image and mapping images of (b) carbon, (c) molybdenum, and (d) sulfur (scale bar: 2  $\mu$ m).

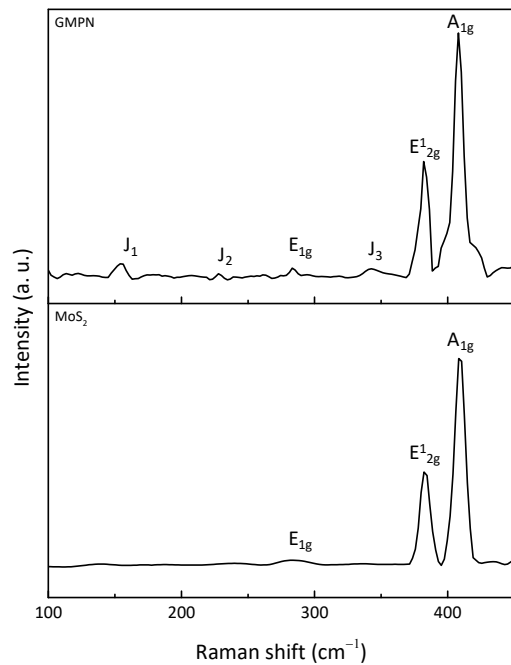


Figure S6. Raman spectra of pristine MoS<sub>2</sub> and GMPN for observing specific peaks related to 1T-MoS<sub>2</sub>.

Table S1. Elemental analysis data of GMPN and controls.

Sample	Element % (measured value)			Element % (calculated value)		
	N	C	S	N	C	S
GMPN	2.760	45.646	10.391	2.275	54.326	12.511
MPN	2.319	16.298	29.541	2.275	37.018	19.815
GPN	4.601	75.313	2.947	2.275	71.634	5.206
GMN	0.131	36.799	0.185	0.000	45.000	18.992

Table S2. Elemental analysis data of GMPNs with different graphene contents.

G:M:P	Element % (measured value)			Element % (calculated value)		
	N	C	S	N	C	S
1:1:80	2.760	45.646	10.391	2.275	54.326	12.511
2:1:80	2.011	64.510	10.637	1.908	60.080	10.493
3:1:80	1.375	71.075	8.785	1.643	64.235	9.035

Table S3. Elemental analysis data of GMPNs with different MoS<sub>2</sub> contents.

G:M:P	Element % (measured value)			Element % (calculated value)		
	N	C	S	N	C	S
1:1:80	2.760	45.646	10.391	2.275	54.326	12.511
1:2:80	1.514	36.902	21.998	1.908	45.564	16.619
1:3:80	1.370	30.582	25.141	1.643	39.235	19.586

Table S4. Elemental analysis data of GMPNs with different PANI-solution contents.

G:M:P	Element % (measured value)			Element % (calculated value)		
	N	C	S	N	C	S
1:1:20	1.082	48.996	18.474	1.056	49.330	15.983
1:1:40	1.805	49.356	17.191	1.643	51.735	14.311
1:1:60	2.241	48.612	17.066	2.016	53.266	13.247
1:1:80	2.760	45.646	10.391	2.275	54.326	12.511

### Quantitative analysis of individual components in the nanohybrids

The nitrogen, carbon, and sulfur contents of the samples were used to infer the composition of the nanohybrids, corresponding to the amount of graphene, MoS<sub>2</sub>, and PANI with dopants, respectively (Table S1–S4). Several assumptions were made in the calculation of the composition of the nanohybrids: 1) graphene constitutes only carbon atoms, 2) PANI has six carbon atoms and a nitrogen atom in its structure, 3) the dopants, DBSA, CSA, and D-sorbitol used to enhance the performance of PANI are also considered, 4) two sulfur atoms are counted in calculating the amount of MoS<sub>2</sub>. As seen Table S1, the difference between the measured elemental data (left) and calculated elemental data (right) for GPMN was insignificant compared with that of the other nanohybrids. This is because the ternary materials interacted strongly and were not permeated with solvent during the filtration process. However, the calculated and measured elemental data for GMN differed significantly because the interaction of graphene and MoS<sub>2</sub> was weak; thus, there was some loss of MoS<sub>2</sub>. Therefore, the composition of GMPN matches the calculated composition more closely than that of the binary nanohybrids. Furthermore, the elemental analysis data for the GMPN samples with different compositions (Table S2 to S4) show that even though duplicate measurements did not exactly coincide with the calculated values, there was acceptable correspondence. In other words, the composition of the GMPN samples with different graphene, MoS<sub>2</sub>, and PANI contents is persuasive.

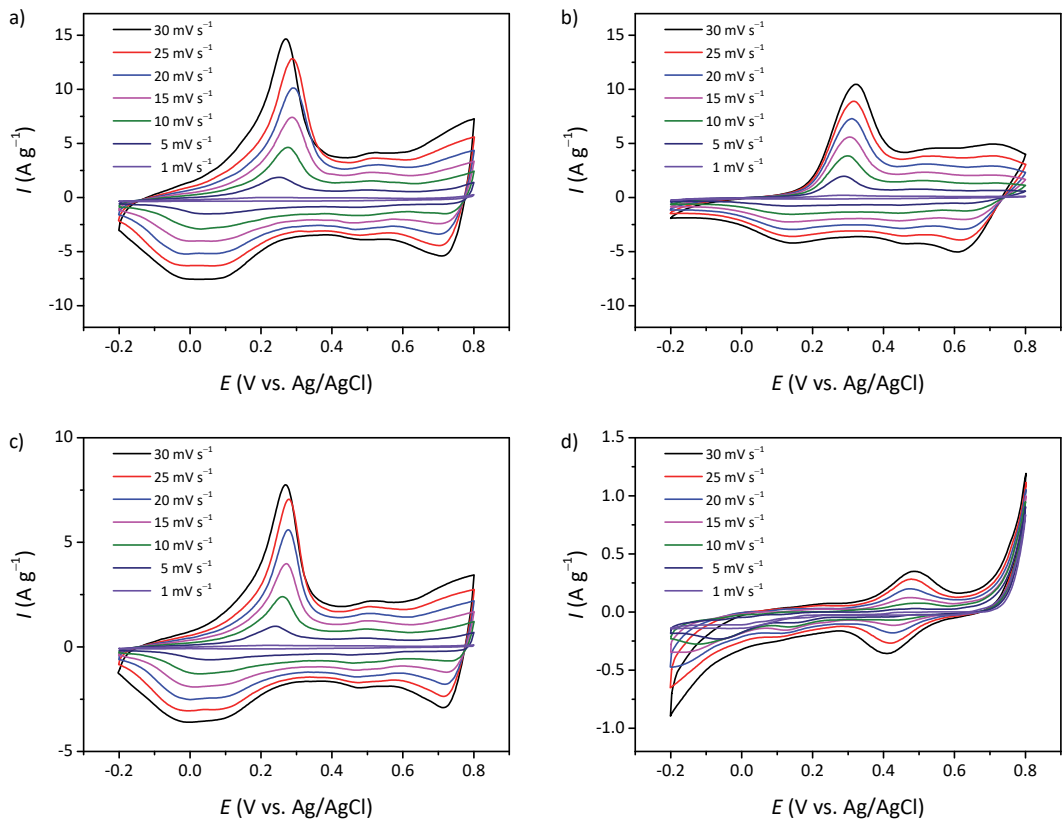


Figure S7. Electrochemical properties of (a) GMPN, (b) MPN, (c) GPN, and (d) GMN at different scan rates in 1 M sulfuric acid.

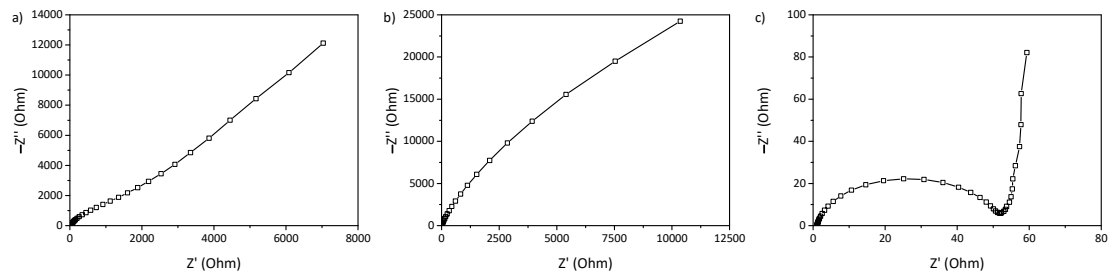


Figure S8. EIS Nyquist plots of components: (a) graphene, (b) MoS<sub>2</sub>, and (c) PANI measured in 1 M sulfuric acid.

Table S5.  $R_{ct}$  of nanohybrids calculated from Figure 5a.

Sample	$R_{ct}$ [ $\Omega$ ]
GMPN	11.72
MPN	48.71
GPN	8.63
GMN	5.42

Table S6.  $R_{ct}$  of nanohybrids calculated from Figure 5b.

G:M:P	$R_{ct}$ [ $\Omega$ ]
1:1:20	26.1
1:1:40	21.42
1:1:60	17.37
1:1:80	11.72
1:1:100	13.29

Table S7.  $R_{ct}$  of nanohybrids calculated from Figure 5c.

G:M:P	$R_{ct}$ [ $\Omega$ ]
0.5:1:80	9.94
1:1:80	11.72
1.5:1:80	14.45
2:1:80	15.32
2.5:1:80	16.66
3:1:80	18.91

Table S8.  $R_{ct}$  of nanohybrids calculated from Figure 5d.

G:M:P	$R_{ct}$ [ $\Omega$ ]
1:0.5:80	8.41
1:1:80	11.72
1:1.5:80	14.12
1:2:80	20.46
1:2.5:80	22.78
1:3:80	38.22

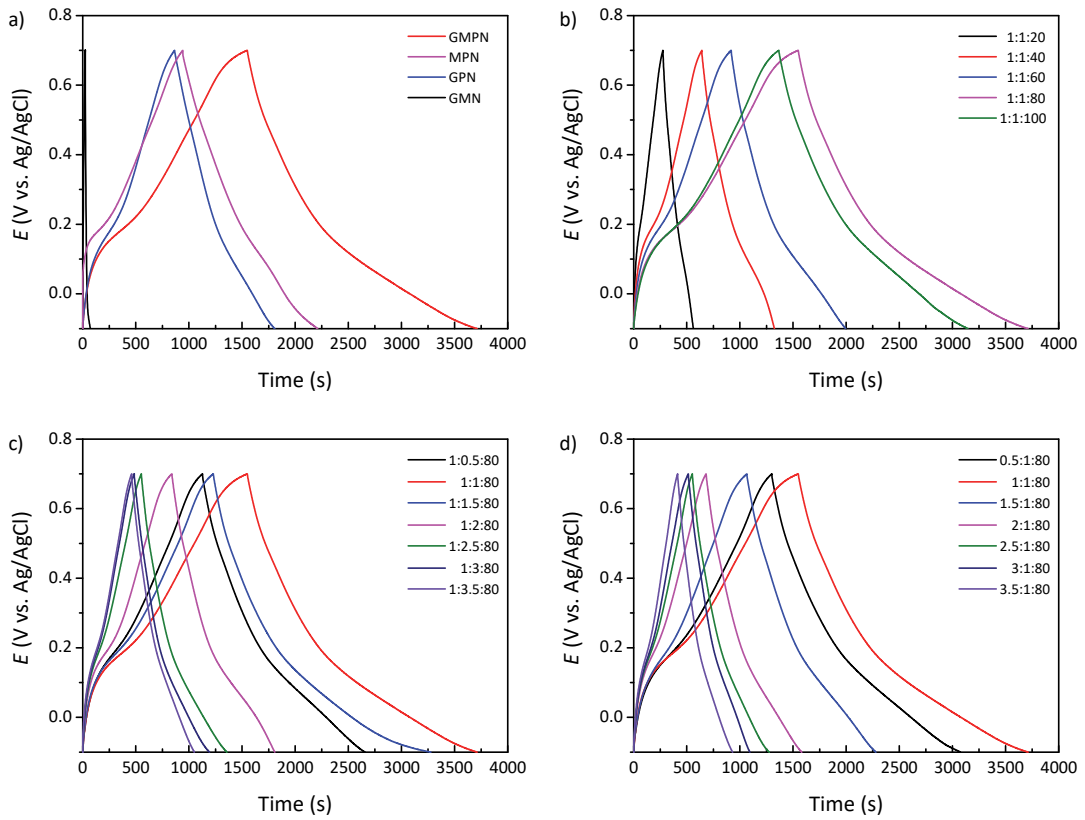


Figure S9. Galvanostatic charge/discharge curves of (a) GMPN and controls, (b) GMPNs with different PANI-solution contents, (c) GMPNs with different graphene contents, and (d) GMPNs with different  $\text{MoS}_2$  contents at a current density of  $0.1 \text{ A g}^{-1}$  in 1 M sulfuric acid.

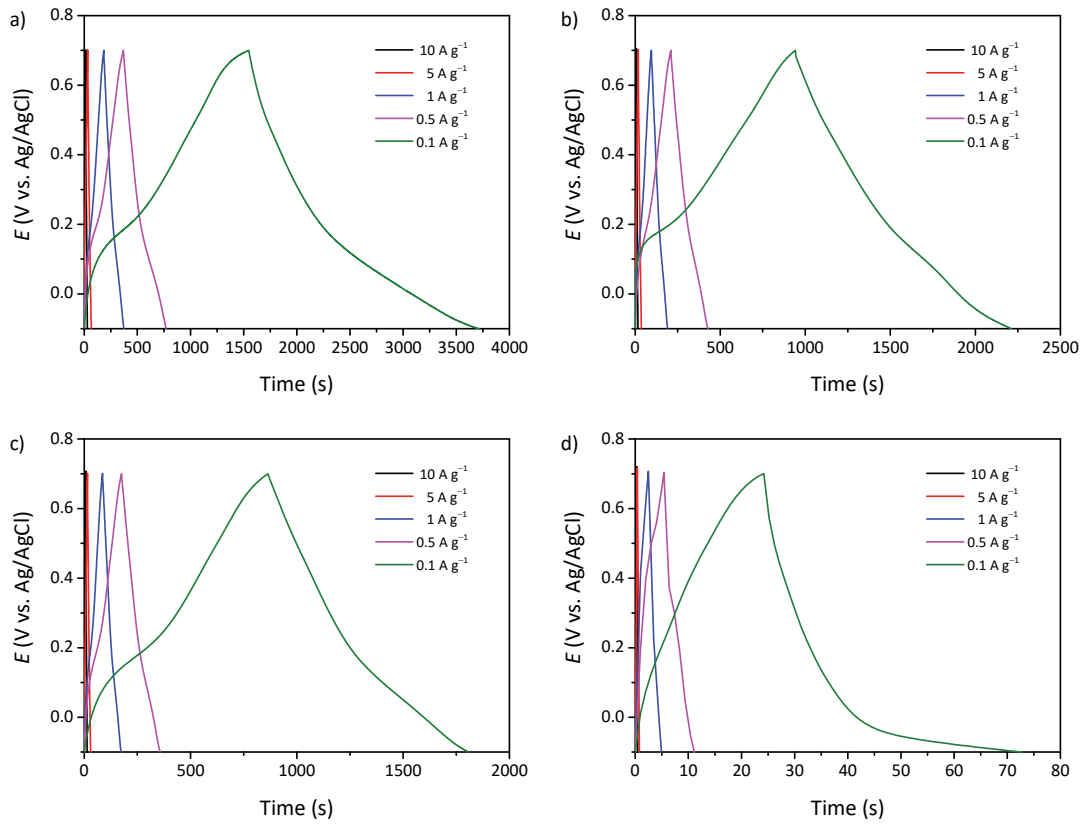


Figure S10. Galvanostatic charge/discharge curves of (a) GMPN, (b) MPN, (c) GPN, and (d) GMN at different current densities in 1 M sulfuric acid.

Table S9. Specific capacitances of nanohybrids at a current density of  $0.1 \text{ A g}^{-1}$ , obtained from Figure 6a.

G:M:P	Capacitance [F g <sup>-1</sup> ]
1:1:20	36.68
1:1:40	81.77
1:1:60	138.43
1:1:80	270.46
1:1:100	229.33

Table S10. Specific capacitances of nanohybrids at a current density of  $0.1 \text{ A g}^{-1}$ , obtained from Figure 6b.

G:M:P	Capacitance [F g <sup>-1</sup> ]
0.5:1:80	221.08
1:1:80	270.46
1.5:1:80	154.33
2:1:80	113.89
2.5:1:80	94.36
3:1:80	81.22

Table S11. Specific capacitances of nanohybrids at a current density of  $0.1 \text{ A g}^{-1}$ , obtained from Figure 6c.

G:M:P	Capacitance [F g <sup>-1</sup> ]
1:0.5:80	191.67
1:1:80	270.46
1:1.5:80	255.15
1:2:80	125.68
1:2.5:80	102.22
1:3:80	90.90

Table S12. Specific capacitances of nanohybrids at a current density of  $0.1 \text{ A g}^{-1}$ , obtained from Figure 6d.

Sample	Capacitance [F g <sup>-1</sup> ]
GMPN	270.46
MPN	155.08
GPN	113.17
GMP	6.23

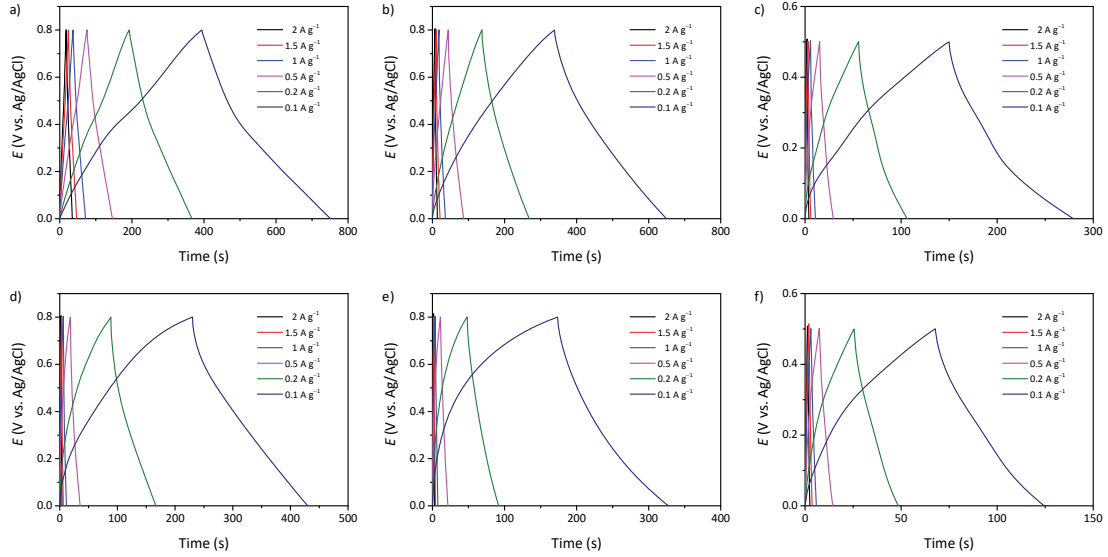


Figure S11. Galvanostatic charge/discharge curves of two-electrode cells exploiting GMPN as an electrode material with different electrolytes, separators, and current collectors at different current densities: using a cellulose separator with (a) 1 M  $\text{H}_2\text{SO}_4$  electrolyte, (b) 1 M  $\text{Na}_2\text{SO}_4$  electrolyte, and (c) 6 M KOH electrolyte; using a polypropylene separator with (d) 1 M  $\text{H}_2\text{SO}_4$  electrolyte, (e) 1 M  $\text{Na}_2\text{SO}_4$  electrolyte, and (f) 6 M KOH electrolyte.

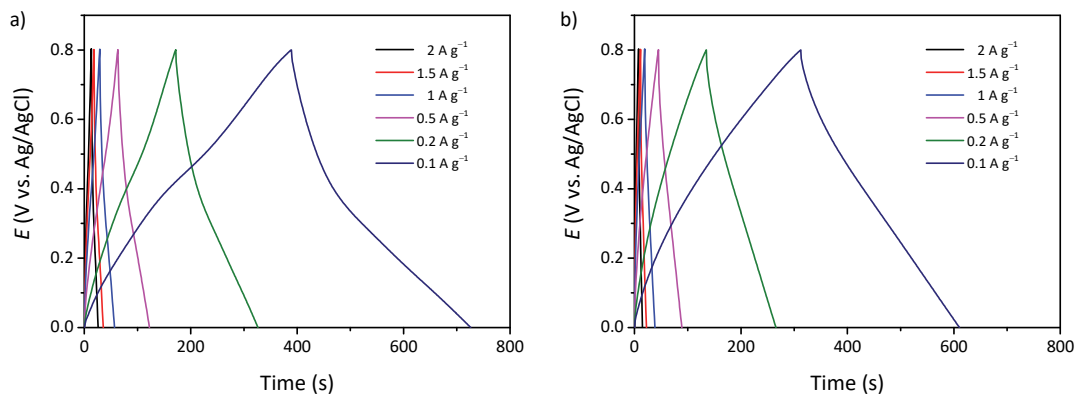


Figure S12. Galvanostatic charge/discharge curves of the flexible all-solid-state GMPN cells consisting of gel electrolytes of (a) PVA/H<sub>2</sub>SO<sub>4</sub> and (b) PVA/Na<sub>2</sub>SO<sub>4</sub> at different current densities.